Exploring novel downstream strategies for the purification of enveloped VLPs

Mafalda Moleirinho[a]

[a] Master student in Biological Engineering Instituto Superior Técnico, Universidade de Lisboa, Av. Rovisco Pais, 1, 1049-001 Lisboa, Portugal.

Abstract: Virus-like particles (VLPs)-based vaccines are promising candidates for the future, offering new perspectives in vaccine development. VLPs applications go beyond new vaccine development, and are applied in targeted drug delivery or in molecular imaging to be used as diagnostics.
In the first part of this work it was improved the state-of-the-art of VLPs purification by evaluating essential but less studied operation – clarification. As a proof-of-concept, the clarification studies were performed for two enveloped VLPs - Influenza and Hepatitis C. The combination of depth filters worked for both VLPs. Reduction of turbidity was achieved and also 100% of recovery yield was obtained in some clarification experiments. The second part of this work reports a two-step approach enabling the in vivo site-specific functionalization of complex enveloped Influenza virus-like particles (VLPs). The initial step involves selective incorporation of the noncanonical azidohomoalanine into nascent hemagglutinin proteins. The second step uses copper free click-chemistry to fluorescently label Influenza VLPs with an Alexa probe. This strategy has no impact on VLP production and purification processes and the biological function is preserved. Azidohomoalanine incorporation, labeling and VLP characterization was monitored and optimized using confocal microscopy and flow cytometry analysis. FACS allowed a refined discrimination/separation between VLP and baculovirus as visualized by atomic force microscopy. A valuable tool for downstream processing monitoring is reported. The versatility and flexibility of this approach offers the possibility of development of multifunctionalized selective particles that can have an important impact on disease targeting (cancer), vaccine/antigen formulations and drug development (drug delivery, diagnostics).

Keywords: clarification, depth filtration, bioconjugation, click chemistry, downstream processing, enveloped Virus-like particles

Introduction

Early vaccine formulations (live or attenuated) are no longer considered the most appropriate for the current needs. Virus-like particle (VLP)-based vaccines are promising candidates for the future, offering new perspectives in vaccine development [1]. VLPs are viral proteins that have the ability to self-assemble into highly ordered repetitive structures empty of DNA. VLPs have been used as vaccines over the last decade [2-4] and there are already approved human vaccines against Hepatitis B and human Papillomavirus viruses that use recombinant VLPs as antigen [1, 5]. Moreover, engineered VLPs carry additional promise of important developments in biomedicine and biotechnology. Their applications go beyond new vaccine development, and are applied in targeted drug delivery or in molecular imaging to be used as diagnostics [6]. Previous studies describe VLPs as a safe and efficient system to deliver functional proteins into cells and that these particles are able to interact with appropriate cell receptors and induce the desired cell stimuli [7]. Genetic engineering of VLPs allowed to explore viral capsids as drug delivery systems [8] that target and selectively treat tumors [9]. Being such a versatile bio-platform, a strategy to chemically modify adenoviral vectors (using Click chemistry) without involving genetic modification has been recently reported [10]. This approach is simpler, more efficient, less time consuming and cost-effective. It not only potentiates VLPs biological applications but it may help on optimizing VLPs production protocols. However, this straightforward route has only been reported for simple non-enveloped VLPs [10]. The increasing constraints of regulatory agencies led to tighter and higher control of biophamarceuticals quality and safety, quantification, characterization and process monitorization, which requires the development of new analytical, more efficient and cost-effective downstream processing (DSP) methods [11-13]. Cell removal and clarification are the interface of up- and down-stream and are also directly affected by increases in biomass. Therefore, the development of robust and consistent depth filters with the capacity to protect more vulnerable downstream membranes is a key target for optimization. Clarification by depth filter is a technology easily scalable, capable of removing soluble impurities and suspended solids.
Hereby a successful site-specific functionalization and labeling of complex enveloped Influenza VLPs within live cells using Click chemistry technology is reported [14-15]. VLPs were produced using the Baculovirus Expression Vector System, increasing DSP complexity [16-17]. The approach here reported enhances the potential applications for these biological molecules not only in terms of drug targeting and advanced biopharmaceuticals development but also as a powerful tool for DSP innovation.

Materials and Methods

Clarification studies

The clarification performance of different filters (already commercialized or prototypes) was evaluated for Influenza and Hepatitis C VLPs, as a proof-of-concept. The devices were kindly provided by Dr. Alex Xenopoulos (R&D Operations, EMD Millipore Corporation, USA) and were set up according to the manufactures' instructions. Briefly, a Tandem 1081 Pump (Sartorius Stedim Biotech, Germany) was used to feed the clarification device with the bioreactor bulk. MasterFlex® 14 tubing (MasterFlex Group, Germany) with 1.6 mm internal diameter was used. The pressure was monitored at the feed inlet by in-line pressure transducers (SciLog®, USA). The clarified volumes were monitored using a technical scale (Sartorius Stedim Biotech, Germany). The filters were previously conditioned with three capsule volumes of buffer 50 mM HEPES, pH 7.4, 300 mM NaCl (working buffer). Filter characteristics and flow rates used are present in table 1.

Table 1 - Filter characteristics and feed flow rates used.

Filter	Pore size (μm)	Filter area (cm^2)	Feed flow rate (mL/min)
Type B	5	17.7	80
Type C	0.3	17.7	80
Type D	-	23	7
Type E	1.2/0.5	17.7	80
Type F	1.2	17.7	80
Type G	2.0/1.2	17.7	80
Type H	0.5	17.7	80
Type I	1.0/1.2	17.7	80
Type J	-	23	7
Type K	-	23	7
Type L	0.22	17.7	80

Cell culture

High Five cell line (Trichoplusia ni derived BTI-Tn-5B1-4) was obtained from Invitrogen (Invitrogen Corporation, Paisley, UK). Cells were routinely cultured in ESF921 protein-free medium (Expression Systems, USA) in 125 mL Erlenmeyer flasks (Corning, USA) with a working volume of 10 mL. High Five cells were kept in a humidified incubator at 27°C and 110 rpm. Every 3-4 days, after reaching a cell concentration of 2-3×10^6 cells/mL they were re-inoculated at 3×10^5 cells/mL. Cell concentration and viability were determined by haemocytometer cell counts (Brandt, Wertheinmain, Germany) and trypan blue exclusion dye method (Merck, Darmstadt, Germany).

VLP production and metabolic labeling optimization

For production studies, cells were cultured in 500 mL Erlenmeyer flasks (Corning, USA) with a working volume of 50 mL or in 2000 mL Erlenmeyer flasks (Corning, USA) with a working volume of 250 mL. High Five cells infection with recombinant baculovirus (kindly provided by Redbiotec AG) encoding *Influenza A/Johannesburg/33/94* HA and M1 proteins was performed at a cell concentration at infection (CCI) of 2×10^6 cells.mL^{-1},with a multiplicity of infection (MOI) of 15 IP.cell^{-1}. After 12 hours post-infection (hpi) the culture medium was removed by centrifugation at 200 g for 10 min and the cells were washed with D-PBS (Gibco®, UK). ESF921 methionine deficient and protein-free medium (Expression Systems, USA) was then added to the infected cells. Noncanonical amino acid incorporation was tested at several hpi values (18, 24, 36 and 42 hpi) in order to identify the best condition for labelled VLP production. The culture medium was supplemented with 4 mM Azidohomoalanine (AnaSpec, USA). To generate appropriate controls, this study also carried out with 4 mM L-Methionine (SIGMA-ALDRICH®, Switzerland) at the same conditions.

Harvest and Clarification

High Five infected cells were harvested at 48 hpi by centrifugation at 200 g for 10 min (JA10 rotor, Avanti J25I centrifuge, Beckman Coulter, USA). The pellet was discarded and Benzonase® (Merck Millipore, Germany) was added to the supernatant at a final concentration of 50 U.mL^{-1} and incubated at room temperature (22°C) for 15 min. The clarification of supernatant was performed by dead-end filtration using a Sartopore® filter with 0.45+0.2 µm pore size (Sartorius, Germany). The clarification of VLP-containing bulk was performed at a constant flow rate of 100 mL/min using a Tandem 1081 Pump (Sartorius Stedim Biotech, Germany). The pressure was monitored by an in-line pressure transducer (SciLog®, USA) to control possible overpressure. The filtration module was previously conditioned with three capsule volumes of buffer 50 mM HEPES, pH 7.4, 300mM NaCl (working buffer).

Anion exchange chromatography

Sartobind® Q MA 75 (Sartorius, Germany) membrane adsorber was used as a first purification step, operated in negative mode (flow through (FT)). The membrane adsorber was equilibrated with 50 mM HEPES, pH 7.4, 400 mM of NaCl equilibration buffer. The VLP clarified suspension was diluted with concentrated NaCl buffer to match the conductivity of equilibration buffer. The flow rate was set to 4.76 MV/min (membrane volume/min) and the VLPs were collected in the FT pool. A final elution step was performed with 50 mM HEPES, pH 7.4, 1.0 M NaCl elution buffer in order to guarantee that all particles were removed from the membrane adsorber. VLP concentration along these fractions was determined by hemagglutination assay and nanoparticle tracking analysis. All chromatographic steps were performed at room temperature (RT) (22 °C).

Ultrafiltration/Diafiltration

Sartobind® Q FT pool containing VLPs were concentrated using tangential flow filtration (TFF). Ultrafiltration experiments were conducted using flat sheet Pellicon XL Ultrafiltration Module Biomax 300 kDa 0.005 m^2 (Merck Millipore, USA).The membrane module was set up accordingly with the manufacturer's instructions. The ultrafiltration module was preconditioned with deionized water, to eliminate trace preservatives and equilibrated with

working buffer before the concentration step. To ensure sterility, the TFF system was sanitized with 0.1 M NaOH and incubated with this solution for 60 min. A Tandem 1081 Pump (Sartorius Stedim Biotech,Germany) was used on the feed side set up to a fixed flow rate of 40 mL/min. Transmembrane pressure (TMP) was controlled by adjusting the retentate flow rate using a flow restriction valve. The pressure was monitored at feed inlet, retentate outlet and permeate outlet by in-line pressure transducers (SciLog®, USA). The permeate volume was monitored using a technical scale (Sartorius Stedim Biotech, Germany). At a proper concentrate volume, three diafiltration volumes with working buffer were performed. After achieving the desired concentration factor, the TFF loop was completely drained and the VLP retentate was recovered. Samples of the final retentate and permeate were taken to assess process yield.

Size exclusion chromatography

Concentrated VLPs were labeled with 20 μM of Alexa Fluor® 488 (Life Technologies, USA) for 60 min, according to manufacturers' instructions and prior to the polishing step. Size exclusion chromatography was performed using a HiLoad 16/600 Superdex 200 pg column (GE Healthcare, USA) coupled to an ÄKTA explorer 10 liquid chromatography system (GE Healthcare, U.K.) equipped with UV and conductivity/pH monitors. System operation and data gathering/analysis was done using the UNICORN™ 5.0 software (GE Healthcare, U.K.). The column was loaded with 5 mL of concentrated VLPs, using a 5 mL capillary loop, at a constant flow rate of 0.5 mL/min. Working buffer was used as eluent and the eluted fractions were collected for further analyses. Elution of Influenza VLPs was monitored online at a wavelength of 234 and 494 nm (emission wavelength of Alexa Fluor® 488).

Hemagglutination assay

Hemagglutinin protein was quantified using a hemagglutination assay. The assay was carried out based on the protocol described elsewhere [18] with some modifications. Briefly, 25 μL of D-PBS (Gibco®, UK) were added in each well of a clear, V bottom 96-well microtiter plate (Sterilin, USA). In the first well (upper left), 25 μL of each sample were added and then two fold serial dilutions (25 μL of sample in an equal volume of PBS) were performed. The excess 25 μL from the final dilution were discarded. After this step, 25 μL of 1% chicken erythrocytes (LOHMANN TIERZUCHT GmbH, Germany) was added to each well of each serial dilution series. The plate was incubated at 4°C for 30 minutes without disturbance. As a positive control, Influenza vaccine (Influvac®, Abbott, USA) was used. The level of hemagglutination was inspected visually for all the wells and the highest dilution capable of agglutinating chicken erythrocytes was determined.

Hepatitis C VLPs quantification

Hepatitis C VLPs were quantified following Gag p30 protein content in process samples using a commercially 154 available QuickTiter MuLV core antigen ELISA kit (MuLV p30) according to the manufacturer's 155 instructions (Cell Biolabs, USA).

Total Protein Quantification

Total protein was quantified using the BCA Protein Assay Kit (Thermo Fisher Scientific, USA) according to the manufacture's protocol. Bovine serum albumin (BSA) was used for the calibration curve (Thermo Fisher Scientific, USA). In order to avoid matrix interference, the samples were diluted between 2-256 fold. The assay took place in a clear 96-well microplate (Nunc,USA) and the absorbance at 562 nm was measured on Infinite® 200 PRO NanoQuant (Tecan, Switzerland) microplate multimode reader.

Total dsDNA Quantification

Total DNA was quantified using the fluorescent-based Quant-iT™ Picogreen® dsDNA assay kit (InvitrogenTM, UK) according to the manufacturer's instructions. In order to avoid matrix interference, the samples were diluted between 2–256 fold with the provided reaction buffer. The assay took place in a black 96-well microplate, flat transparent (Corning, USA) and the fluorescence was measured on Infinite® 200 PRO NanoQuant (Tecan, Switzerland)microplate multimode reader.

Nanoparticle tracking analysis

Total virus-like particles concentration and size distribution were measured using the NanoSight NS500 (Nanosight Ltd, UK). The samples were diluted in D-PBS (Gibco®, UK) so that virus-like particles concentration would be in the 10^8–10^9 particles mL^{-1} – the instrument's linear range. All measurements were performed at 22 °C. Sample videos were analyzed with the Nanoparticle Tracking Analysis (NTA) 2.3 Analytical software - release version build 0025. Capture settings (shutter and gain) were adjusted manually. For each sample 60-seconds videos were acquired and particles between 70 and 130 nm were considered.

Baculovirus particles quantification

Baculovirus viral DNA was extracted and purified using the High Pure Viral Nucleic Acid Kit (Roche Diagnostics, Germany) using the manufacturer's instructions. The number of genome containing particles were monitored by real time quantitative PCR (q-PCR) following the protocol described elsewhere [19].

Confocal Microscopy

Using Life Technologies (Carlsbad, CA, USA) Tetraspeck™ beads one can use as visual reference of successful VLP labeling and detection. Due to its four –color fluorescence using green (which also detects labeled VLP) and orange (specific for beads) one can perform quantitative analysis on the detected VLP. An inverted confocal point-scanning Zeiss LSM 710 microscope

equipped with 405, 458, 488, 561 and 633 nm lasers. Due to the diffraction limit associated with microscopy techniques, no particle below that threshold can be visualized with high resolution. Thus it would appear the point-spread function (PSF) of the instrument. VLP are sub-diffraction limit particles, thus their signal in the microscope would be the PSF of the microscope (approx. 240 nm). By using 500 nm fluorescent beads as a control, together with their dual-fluorescence emission spectra, one can perform an accurate detection of sub-diffraction limit particles – VLP. This methodology was used to evaluate the best time for AA addition after baculovirus infection: 12, 24, 36 and 48 hpi were evaluated. 100-fold dilutions of each condition supernatant were deposited into IbiTreat 8 µ-well slides (Ibidi, Martinsried, Germany) and allowed to attach for 1h. Each preparation was then labeled with 20 µM of Alexa Fluor® 488 (C-10405, Life Technologies, USA) or 30 min, according to manufacturers' instructions. The sample was washed 3 times with PBS and 500-fold dilution of 500 nm fluorescent beads were added to each sample for 30 min. Medium was changed for fresh PBS. In all steps, the PBS used for dilution preparation, wash steps and sample acquisition, was filtered with a 0.1µm nylon filter. Control VLP (methionine AA added during VLP production, SIGMA-ALDRICH®, Switzerland), modified VLP (with the Click-it noncanonical AA, Azidohomoalanine, AnaSpec, USA), and 500 nm beads were imaged using a 63x-oil objective and green and orange channels were acquired. ImageJ [20] software was used to merge images and to perform particle size distribution analysis in each preparation from which the full width at half maximum was determined (reflects average particle size).

Flow Cytometry

Detection and characterization of labeled VLP and size discrimination between VLP (spheres of 100-200 nm) and Baculovirus (rods of 200-400 nm) with flow cytometry were performed using a BD LSR Fortessa (BD Biosciences, San Jose, CA, USA). It is equipped with 3 lasers (violet—405 nm, blue—488 and red—640 nm), forward and side scatter detectors and 9 fluorescence emission detectors (530/30 – green channel was used for VLP-A488 and 100, 200 and 500 nm Tetraspeck fluorescent beads. Side scatter detector was used to define the detection threshold. Using 100, 200 and 500 nm beads one can build a particle size ruler in flow cytometry with the scatter signal [21] which can then be used to evaluate the VLP samples size distribution. The refractive index (RI) depends on the material of the scattered solution, thus direct correlation of bead size and VLP can only be achieved if each sample has approximately the same RI. The RI for PBS, UF Retentate, SEC fractions (100-fold dilution), Baculovirus (100-fold dilution), 100 nm (2000-fold dilution), 200 nm (1000-fold dilution) and 500 nm beads (500-fold dilution are respectively, 1.334, 1.335, 1.335, 1.336, 1.334, 1.334, 1.334, measured using a digital refractometer (AR 200 Digital Refractometer, Leica, USA). The side-scatter/alexa-488 correlograms were acquired for each bead and VLP sample at the dilutions previously stated to detect baculovirus presence and further evaluate particle separation by sorting. In all steps, the PBS used for dilution preparation, wash steps and sample acquisition, was filtered with a 0.1 µm nylon filter.

VLP sorting

Sorting of the SEC F4 sample from the downstream processing was performed to separate VLPs from the baculovirus-rich fraction (> 200 nm). Fluorescence activated sorting was performed in a BD FACS Aria III equipped with 3 lasers (blue - 488 nm, yellow-green – 561 nm and red – 633 nm). 200 nm fluorescent beads were used to define two sorting populations: P2 corresponding to the > 200 particles detected, which is a baculovirus-rich population and P1 which is the < 200 nm particles that, in contrast to P2 is VLP-rich. Each population was acquired in vials filled with PBS and the presence for VLP and baculovirus was performed by atomic force microscopy.

Atomic force microscopy

AFM images of VLPs and baculovirus were acquired using a JPK Nano Wizard II (Berlin, Germany) mounted on a Zeiss Axiovert 200 inverted microscope (Göttingen, Germany). The AFM head is equipped with a 15-µm z-range linearized piezoelectric scanner and an infrared laser. All samples were prepared in freshly cleaved mica. For scanning in liquid environment the mica was pretreated with poly-D-lysine for 20 minutes and rinsed with mili-Q water. A 50 µL drop of each sample was added to the mica and rinsed with PBS buffer at least 4 times. The sample was then allowed to air-dry or maintained in buffer for subsequent imaging. Scanning was performed using uncoated silicon ACL cantilevers from Applied NanoStructure for air-dried samples and uncoated silicon cantilevers HQ:CSC38 /No Al from MikroMasch for samples in liquid medium. ACL cantilevers had typical resonance frequencies between 145 and 230 kHz and an average spring constant of 45 N/m. HQ:CSC38 cantilevers had typical resonance frequencies between 5 and KHz and an average spring constant of 0.03 N/m. All measurements were carried out in contact mode. All images were obtained with the same or similar AFM parameters (setpoint, gain and scan rate) values. Setpoint and gain were continuously adjusted during scanning to maintain the lowest possible value and reduce sample damage.

Transmission Electron Microscopy

To analyze the presence, integrity and morphology (shape, size) of the VLPs, electron microscopy was performed as follows: a drop (5 µL) of sample was adsorbed onto a formvar coated 150 mesh copper grid from Veco (Science Services, Germany) for 2 minutes. The grid was washed 5 times with sterile filtered dH2O. Then it was soaked in 2% uranyl acetate for 2 minutes and dried in air at room temperature (22°C). The samples were examined

with a Hitachi H-7650 120 Kv electron microscope (Hitachi High-Technologies Corporation, Japan).

Results and discussion I

The main goal of clarification step using depth filters is to obtain maximal product yield and reduce impurities (reduce turbidity, DNA and if possible, baculovirus). To optimize the first step of downstream process, a scheme of different depth filter conjugations for Influenza and Hepatitis C VLPs is presented. Depth filters are designed to remove particle impurities throughout the porous media and were used to directly process cell culture suspensions although, filter type L were examined for the filtration of a VLP harvested by centrifugation. To evaluate filter performance samples were taken from the feed and the filtrate of each run. The samples were analyzed with respect to HA activity, turbidity, total protein, Gag p30 protein content and DNA (see Table 2). Yield coefficients were calculated as the ratio of concentrations or activities (filtrate over feed). Similar loading volume of VLP supernatant and flow conditions were used in order to established comparison between filters.

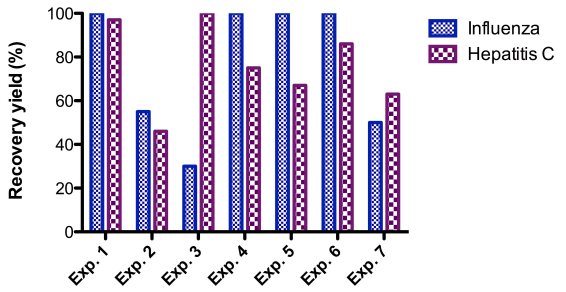

Figure 1 - Comparative evolution of different filter combination for clarification of Influenza and Hepatitis C produced in insect cell culture. For Influenza and Hepatitic C the recovery yields were based on HA and Gag p30 protein content, respectively.

Figure 1 shows similar recovery yields between Influenza and Hepatitis C VLPs for clarification tests number 1, 2, 6 and 7. The main differences are in test number 3 which had a lower recovery yield for Influenza than Hepatitis C. This can be due to the fact that Influenza VLPs are budding VLPs (such as Hepatitis C) and, hemagglutinin is incorporated at high cell density into apical cell membranes after infection. Accordingly, fragments of the cell membranes are likely to posses HA activity similar to the VLPs. The main limitation of the HA assay is that HA activity of VLPs and the activity of fragments of the cell membranes cannot be distinguished by the assay. The removal of such fragments by the depth filtration would lead to an apparent reduction of the product yield and could particularly explain the losses in the depth filtration steps. In addiction, as shown in Table 2, these clarification trains led to a significant reduction of DNA (removals between 70-90% of their initial mass) for both types of VLPs. Besides the removal of DNA, the data listed in Table 2 also demonstrates that these filter combinations are able to remove other impurities including baculovirus and reducing turbidity. In clarification train number 5, the turbidity of Influenza supernatant was reduced to 2% by the combination of both filter types D and I while 100% of the product was preserved. For Hepatitis C, although the recovery was slightly lower, the turbidity was reduced to 15% using the same combination of depth filters. Comparing the two VLPs concerning the baculovirus removal, Influenza had LRV higher mean that more baculovirus were removed during the clarification. This can be due to the filtration material which may also retain baculovirus by adsorption, system variations (different cell lines) and the different initial concentration of baculovirus (1.38×10^{12} BV particles/mL for Influenza and 1.91×10^{11} BV particles/mL for Hepatitis C).

Filter types B, G and L blocked and the filtrated volume were lower when comparing with other clarification tests. Considering that, two approaches

Table 2 - Filtration performance for each clarification train based on recovery yields, turbidity and total protein and DNA removal. For Influenza and Hepatitic C the recovery yields were based on HA and Gag p30 protein content, respectively.

Clarification train	Influenza VLPs					Hepatitis C VLPs				
	HA	Turb.[1]	Prot.[2]	DNA[3]	LRV[4]	Gag p30	Turb.[1]	Prot.[2]	DNA[3]	LRV[4]
1 : Type B[5]⟹Type C	100	17	31	83	2.2	97	60	9	72	0.56
2 : Type D⟹Type E	55	2	32	99	3	46	15	17	91	0.89
3 : Type B[5]⟹Type F	30	33	49	79	1.7	100	61	12	72	0.51
4 : Type G[5]⟹Type H[6]	100	7	49	79	2.3	75	20	0	76	0.78
5 : Type D⟹Type I	100	2	22	94	3.1	67	15	10	92	0.9
6 : Type J⟹Type K	100	6	29	84	2.8	86	19	0	85	0.88
7 : Centrifuged⟹Type L[5]	50	4	37	91	2.8	63	14	0	83	1.7

[1] %Remaining turbidity
[2] %Total protein removal
[3] %DNA removal
[4] Log10 of total baculovirus titer (obtained by qPCR) reduction assuming the bulk viral titer as reference.
[5] Lower filter volume due to filter blocked.
[6] For Influenza, clarification train number 4 it was just composed of filter type G.

are possible: the filter pore sizes are small or, the membrane area per volume feed of depth filters needs to be optimized.
A successful clarification of bioreactor bulks was achieved by a combination of depth filters for both Influenza and Hepatitis C VLPs. Reduction of turbidity was achieved and also an acceptable recovery yield was obtained. The most promising filters must have a compromise between high reduction of impurities (turbidity, DNA, protein, baculovirus) and a high VLPs recovery yield. Having this in mind, clarification trains number 5 and 6 for Influenza VLPs and Hepatitis C VLPs are those that showed the best performance, respectively.

Results and discussion II

The site-specific *in vivo* VLP modification and labeling was achieved by a two-step approach. The first step involves the metabolic incorporation of the noncanonical amino acid azidohomoalanine (Aha), a methionine analogue containing an azide group, into hemagglutinin (HA) protein of Influenza VLPs. Azide tagging allows labelling without dramatically changing the physico-chemical properties and biological function of these molecules [14]. The second step is the protein tagging with the desired functionalization. Here, we used an Alexa 488 fluorescent probe for protein labelling, where the tagging molecule binds to the azido moiety of Aha via a chemo selective "click" reaction azide-alkyne. The labeling can be performed at the desired purification step to achieve maximum yields and purified VLPs. Briefly, to produce *in vivo* labeled VLPs, the cells were grown in culture and fed with Aha amino acid during protein synthesis. Canonical methionine (Met) amino acid was added to a parallel cell culture in order to have an appropriate control. During protein synthesis, HA protein incorporates the Aha amino acid. Since HA is a protein from the envelop, VLPs carry the modified amino acid after their budding from the host cells. At this stage is obtained a complex particle that

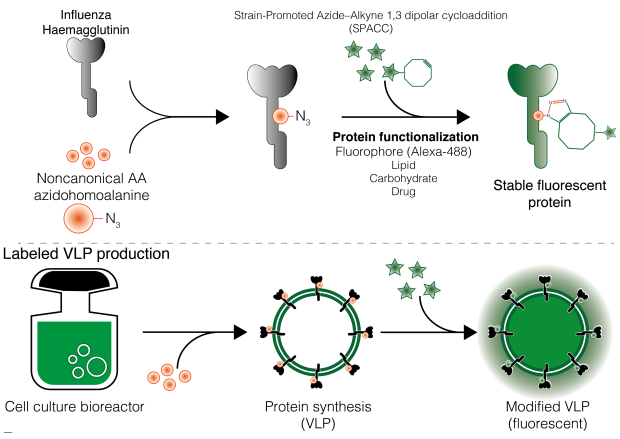

Figure 2 - Site-specific *in vivo* covalent modification and labelling of enveloped Influenza VLPs. Schematic representation of the procedure to introduce a noncanonical amino acid (Aha) prone to perform covalent binding by azide ligation.

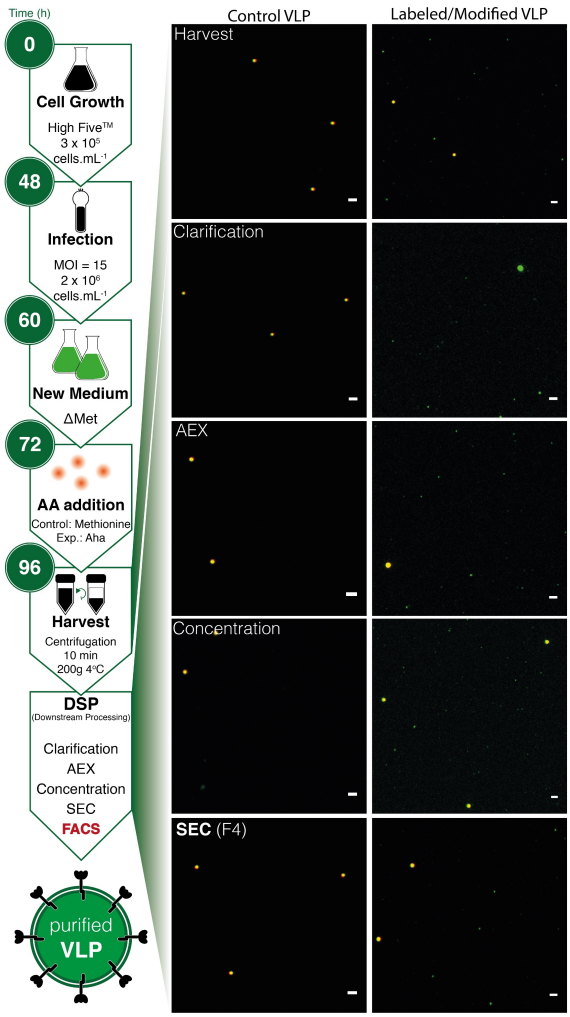

Figure 3 - Flowchart of VLP production and purification steps. In each DSP step, including the fractions acquired in the SEC step, confocal microscopy images were taken in order to monitor the presence of modified VLPs. Scale bars (white) indicate 2 µm in all images.

possess Aha-modified HA in the envelope, prone to be further labeled with a fluorescent probe (Figure 2). The time of addition of amino acids was optimized using small scale (50 mL) batch productions. The incorporation of Aha into HA protein was evaluated at different conditions. 12, 24, 36 and 48 hours post infection (hpi) of cells with baculovirus were evaluated by Nanoparticle tracking analysis (data not shown), confocal microscopy and by flow cytometry analysis. The time of addition that retrieved a higher concentration of fluorescent VLPs was 24 hpi. This was the time that was further used for scale-up (500 mL) Influenza VLP production. Labeling was done after harvesting of the VLPs. 500 nm fluorescent beads were used in confocal microscopy analysis as fiducial markers of size and green fluorescence signal visual reference of successful VLP labeling and detection. Due to its multi-color fluorescence profile, red signal was also acquired. Green-red merged images allowed to discriminate VLPs (green) and beads (yellow) dots, not only by the particle size, but also by its color. With this methodology one can perform quantitative analysis on the detected VLPs. The number per

μm^2 and mean fluorescence intensity (I_f) of labeled-VLPs determined by imaging processing of confocal images may indicate the optimal conditions to perform the functionalization process.
Particles that are below the diffraction limit of the microscope will appear as the point-spread function (PSF) of the instrument. VLPs are sub-diffraction limit particles, thus their signal would be the PSF of the microscope (approximately 240 nm). Particle size analysis was performed and the full width at half maximum (FWMH) was determined, a parameter that is a better approximation to particle size. Control fluorescent beads (size approx. 500 nm) alone present a FWMH value of approximately 540 nm. The mixture between VLPs and beads showed a bimodal size distribution, indicating the presence of both particles. As mentioned, being with sizes bellow the resolution limit of the microscope, their signal limited by the PSF, thus the value observed for the VLP particles has an average size distribution of 240 nm, microscope's PSF. Control VLP sample with methionine addition showed no green fluorescence signal, even after incubation with Alexa probe. This means that incorporation of Aha is necessary to observe fluorescence and that azide ligation between the noncanonical amino acid and the fluorophore is site-specific. 24 hpi was the best time to incorporate Aha into HA protein (one reached approx. 3722 labeled-VLP per cm^2 with an I_f of 670.5±167 *a.u.* (mean ± SD), 40% and 100% higher than 12 hpi or 36/48 hpi, respectively).
The optimization of amino acid incorporation made the system suitable for scale-up production and purification of labelled VLPs (Figure 3). High Five cell culture started at a concentration of 3x10^5 cells.mL^{-1} until reaching a concentration of 2x10^6 cells.mL^{-1}. At this point, approximately 48 h after cell culture initiation, cells were infected with recombinant baculovirus (hpi=0) encoding the H3 subtype A/Johannesburg/33/1994 Influenza virus strain. After 60 h (hpi=12) cell culture medium was replaced by a methionine deficient one. To label mainly the HA protein, addition of Aha amino acid to the cell culture was only performed after the late onset of gene expression (hpi=24). Met was also added at this time to the control cell culture. Harvest of infected cells was performed 48h hpi, when the highest productivity was achieved, a parameter that was screened and optimized previously (data not shown). Cell pellet was discarded and the VLP-rich supernatant collected. DSP proceeded with a standard protocol for Influenza VLP purification, already implemented at the host laboratory. Analysis of all DSP steps to monitor presence and concentration of modified VLP across the process was performed not only by confocal microscopy (Figure 3) but also by flow cytometry (data not shown) for both labelled and control VLPs. Alexa probe was added to the samples before analysis. Clarification of the supernatant, to remove remaining cells and cell debris, was performed using depth filter technology. The intermediate purification comprised an anionic exchange chromatography (AEX) and a concentration/diafiltration step using ultrafiltration technology. AEX was operated in negative (flowthrough) mode, which means that at this step, the working volume is still high. To make the process cost-effective, the labelling with Alexa during the purification process was only performed after concentration of the flowthrough bulk. Size exclusion chromatography (SEC) was used as a polishing step to remove remaining impurities as baculovirus, DNA and host cell proteins (Figure 4) Although SEC removed some baculovirus, after

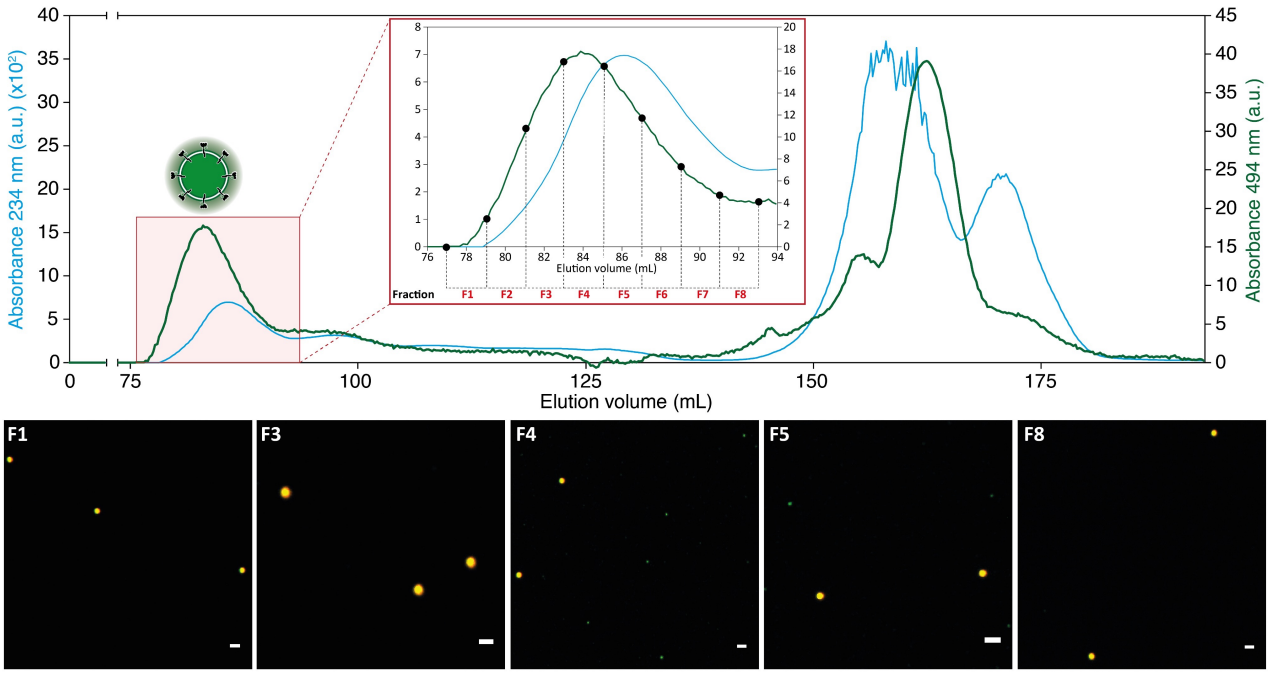

Figure 4 - Detailed interpretation of VLP polishing step using size exclusion chromatography (SEC). The elution profile was followed at 234 nm and at 494 nm (emission wavelength of Alexa probe). VLPs are contained in the column void volume. For each SEC fraction, confocal microscopy images were taken in order to monitor the presence of modified VLP (green fluorescent VLP). Scale bars (white) indicate 2 μm in all images.

this step the product still has this impurity. A Fluorescence-activated cell sorting (FACS) step was added as final step to the process to overcome this issue and separate VLPs from baculovirus according to their distinct particle size (150-200 nm and 300-400 nm, respectively). Further analysis of HA, baculovirus, total protein and DNA concentration was also performed. Polishing step (SEC) (Figure 4) and FACS (Figure 5) will be discussed later on. Moreover, as above mentioned the concentrated Aha-labeled VLP sample showed an I_f of 670.5±167 *a.u.* in the confocal images whereas only background fluorescence intensity levels were detected in the control VLP samples. The residual green signal detected at the control concentration step is mainly due to unspecific binding of the probe (incorporation onto hydrophobic moieties of lipid membranes) to process impurities that are more easily observed at higher concentrations. Furthermore, the concentration detected was residual when compared to the labelled VLPs (data not shown). The data confirmed the presence of labelled VLPs across DSP, with levels of concentration and purity consistent with the evaluated step. Ultrafiltration permeates and column wash fractions from both AEX and SEC were analyzed and no loss of labelled VLP was detected. As proven here, this methodology is a powerful tool to monitor, on-line or at-line, at all steps of the process the product of interest which can play an important role on DSP optimization.

The purification process flowchart was chosen as a proof of concept for the applied methodology, meaning that other schemes and other types of chromatography can also be exploited. As already discussed, labelling was performed prior to SEC step to decrease the process cost. Since the previous chromatographic step was performed in a negative mode, SEC was the step that allowed a fine-tune optimization of the process. Each fraction of this polishing step was interpreted in detail by confocal microscopy (Figure 4) and was also confirmed by flow cytometry analysis (data not shown). Baculovirus rod-shape form makes difficult to distinguish between them and VLPs because even using different detection methods there are angles in which their size look similar. Moreover,

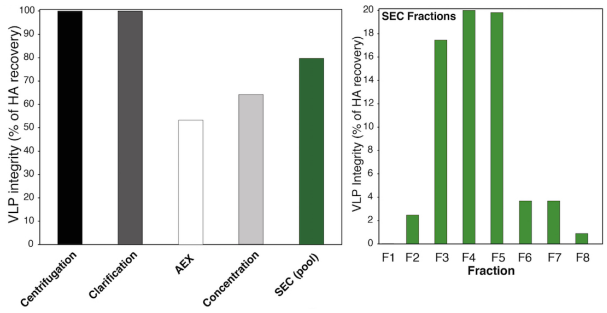

Figure 5 - Integrity and functionality of modified VLPs. A) Hemagglutination assay for each step of modified VLP purification process to assess preservation of HA biological function. B) Hemagglutination assay for each fraction of SEC step.

like VLPs, baculovirus also bud out of the cell leading to an envelope content similar between the two species [22]. Control VLPs were injected onto SEC column and the elution profile was followed at 234 nm (280 and 260 nm were also tested but showed lower absorbance intensity and signal-to-noise ratio). The elution profile of labelled VLPs and control is very similar, with VLPs eluting at the void volume of SEC column as expected (Figure 4). For modified VLP bulk, the absorbance intensity at 494 nm was also evaluated (emission wavelength of Alexa probe). Usually, the VLPs are contained in the void volume peak of the chromatogram due to their high Stoke radius. However, comparing the two wavelengths one can observe that the two peaks are not superimposed. Fraction F4 was the one that presented a higher fluorescence (494 nm) value, which does not correspond to the top peak at 234 nm. Confocal microscopy images also revealed that F4 is the fraction with a higher concentration of labelled VLPs, in accordance with SEC chromatogram and flow cytometry analysis (data not shown). This means that there is a mixture of VLPs and other components eluting in the void volume. Due to its rod-shape, baculovirus elute in different volumes of the chromatogram. The novelty is that this labelling methodology enables a better discrimination between VLPs and other process impurities, in particular baculovirus, the major contaminant of this process. The on-line detection of VLPs lead to a more informed decision on what fractions one should choose to proceed with the purification process. This has an important role in obtaining a higher recovery yield with an elevated level of VLP purity. The peak at the end of the chromatogram corresponds to free probe (494 nm) or DNA and low molecular weight contaminants (234 nm).

Modified VLP integrity and HA biological function were assessed by Hemagglutination assay (Figure 5A; Figure 5B). The principle of this assay is the biological interaction between sialic acid receptors present in erythrocytes and HA protein [23]. The same happens within our conditions, thus proving that the HA biological function is preserved even after chemical modification/functionalization and labelling. The ability of these enveloped VLPs to maintain their characteristics may indicate that this methodology can be used to functionalize these particles with distinct targets. HA content increases as fluorescence intensity increases (Figure 5; Figure 5B) meaning that the labelling is specific for Aha-containing Influenza VLPs. SEC fraction F4 and F5 present the higher percentage of HA recovery which complies with confocal microscopy results (Figure 4) and flow cytometry data (data not shown). TEM analysis was performed to assess presence, integrity and morphology of control (Figure 6A) and modified VLPs (Figure 6B). The morphology is maintained as their size (approximately 170 nm) and spherical shape are similar. Moreover, ultrastructural details of both VLPs' envelope revealed the characteristic Influenza HA spikes. Flow cytometry analysis allowed the detection and characterization of labelled VLPs and the size discrimination between

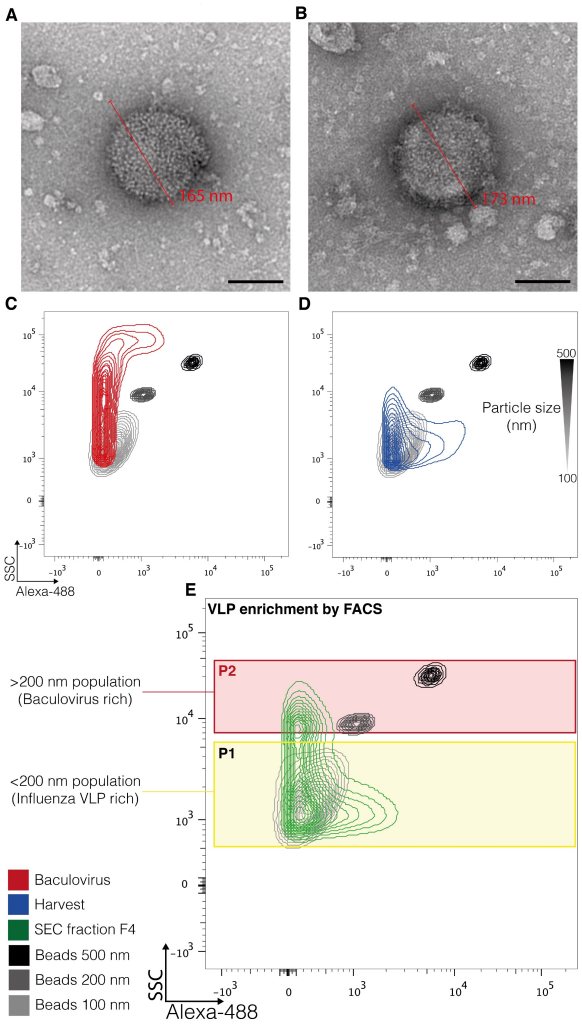

Figure 6 - Integrity and functionality of modified VLPs. A) TEM analysis of control VLPs at the concentration step of the purification process. Scale bar indicates 100 nm. B) TEM analysis of modified VLPs at the concentration step of the purification process. Scale bar indicates 100 nm. C) Flow cytometry of a baculovirus sample This analysis was made to monitor the scatter profile of these 200-400 nm length rod-shape particles (blue) nm. D) Flow cytometry of a VLP sample before the DSP steps (red) showing that there are clearly two particle populations, one green positive population at approx.. 200 nm and one with lower green fluorescence that has an higher size distribution. E) Flow cytometry of fraction F4 from VLP SEC purification step. Taking into account the green fluorescent signal the >200 nm fraction is reduced when compared to E), due to VLP specific green fluorescence signal. This sample was sorted with populations P1 (<200 nm population VLP-rich) and P2 (>200 nm

these particles (spheres of 100-200 nm) and baculovirus (rods of 200-400 nm). Fluorescent beads of 100, 200 and 500 nm were used as a particle size ruler in flow cytometry with the side-scatter signal which can then be used to evaluate the VLP samples size distribution. It is possible to do a direct correlation between bead size and VLP samples since their refractive index is similar.

2D correlogram of side scatter and green fluorescence signals were acquired for each bead (100, 200 and 500 nm), for the VLP and control samples in order to detect baculovirus presence and evaluate further particle separation by cell sorting. A baculovirus sample (used for cell infection and VLP production) was analyzed in order to monitor the scatter profile of these 200-400 nm length rod-shape particles. It is noticeable that sizes ranging from ≈200 to ≈500 nm are observed, indicating that these rod-shapes are very polydisperse. A sample from the harvest step showed that at this stage there are clearly two particle populations, one green positive population at approximately 200 nm and one with lower green fluorescence that has higher size distribution (Figure 6D). Taking into account that this sample is from an early purification step, still rich in baculovirus contamination, this size heterogeneity comes from this VLP/baculovirus mixture. Moving to a fraction from the SEC step (Figure 6E) it is possible to observe that the green fluorescent signal of the >200 nm fraction is reduced when comparing to baculovirus and harvest panels (Figure 6C; Figure 6D). As SEC sample is from a final purification step, baculovirus presence is reduced when compared to VLP. However, SEC fraction still contains baculovirus as they elute across the majority of the chromatogram due to their rod-shape. VLP sorting of the SEC F4 fraction sample was performed to separate VLPs from baculovirus. 200 nm fluorescent beads were used to define two sorting populations: P2 corresponding to the > 200 nm particles detected, which is a baculovirus-rich population and P1 which is the < 200 nm particles that, in contrast to P2 is VLP-rich (Figure 6E). This strategy allowed to increase the yield on VLP production and to minimize baculovirus presence in the final DSP product.

TEM analysis of baculovirus control (used to infect cells) and modified VLP (after concentration) was performed to evaluate the size and possible heterogeneity of samples (data not shown). Baculovirus sample presented a characteristic rod-shape with a normal size of approximately 250 nm. As expected, concentrated VLP sample had both small and larger particles, corresponding to VLPs or baculovirus and process impurities, respectively. VLPs' size is different from the one presented previously (Figure 6A; Figure 6B) which confirms the heterogeneity of the system.

The presence of VLP and baculovirus was performed for baculovirus control, P1 and P2 sorting populations by atomic force microscopy (AFM) (data not shown). Acquired AFM images of baculovirus control samples revealed a well-known rod-shape with small diameter length values. P1 sorting population (<200 nm, VLP rich fraction) images only revealed the presence of spherical particles. On the other hand, P2 sorting population (>200 nm, baculovirus rich fraction) presented only large particles, mainly consisted of baculovirus rod-shaped particles and other large process impurities. Baculovirus size of P2 sorting population is similar to the one from the control.

This data confirmed that our system is suitable for FACS purification step, an important progress in the increasing demand for VLP/baculovirus separation for better attain DSP quality control demands.

Conclusions

Enveloped VLPs play an important role in the current medical therapies and have an enormous potential for the development of new applications in the fields of vaccination and gene therapy.

The upstream process has evolved substantially over the last few decades, on the opposite the downstream processing has been repeatedly identified as the bottleneck in the biopharmaceutical process. Recent efforts have been made in order to improve the downstream processing, but its majority focused on the chromatographic separation. The upstream technology advances enabled high cell densities, however, this and other improvements have created new challenges for bulk clarification. It is also important to mention that the more efficient clarification step is, more robust will be the process and less subject to variations in the upstream.

The clarification trains here evaluated are suggested as an alternative for bulk centrifugation (Results I). A successful clarification strategy of bioreactor bulks was achieved by a combination of depth filters for Influenza and Hepatitis C VLPs and reduction of turbidity was also obtained. In addiction, a first removal of solubles impurities (cell debris and DNA) is achieved and 100% of recovery yield was obtained in some clarification trains. However, batch-to-batch variation of bioreactors caused differences in VLPs yield and level of contaminant depletion.

In the second part of this work, it is reported a straightforward two-step strategy to chemically functionalize and label complex enveloped VLPs in vivo using copper free click chemistry. This flexible and site-specific system does not have an impact on biological function of the studied VLPs and can be potentially used in several virus or VLPs. This approach is simpler, more efficient, less time consuming and cost-effective. The reported strategy can be used for multifunctionalization of these particles, expanding their utility in exciting applications, such as drug delivery or molecular imaging agents for diagnostics. It is a powerful tool for DSP monitoring and optimization, allowing the improvement of product recovery yields and increasing VLP purity levels. Moreover, it is a highly promising method to be applied in new efficient and cost-effective analytical technologies.

Finally, the most straightforward use of VLPs is to use them for vaccination against the virus from which they were derived. Moreover, the enveloped VLPs applications go beyond new vaccine development, and are applied in targeted drug delivery or in molecular imaging to be used as diagnostics, carrying the promise of important developments in the fields of biomedicine and biotechnology. To have an adequate response for all these VLPs applications, an universal DSP for this particles must be design. This is an essential step to create an efficient platform to produce and purify VLPs that are able to fulfill the actual and futures needs of the pharmaceutical industry.

References

[1] Pitoiset, F. & Bellier, B. Enveloped virus-like particle platforms : vaccines of the future ? *Expert Rev. Vaccines* **14,** 913–915 (2015).

[2] Plummer, E. M. & Manchester, M. Viral nanoparticles and virus-like particles: Platforms for contemporary vaccine design. *Wiley Interdiscip. Rev. Nanomedicine Nanobiotechnology* **3,** 174–196 (2011).

[3] Fernandes, F., Teixeira, A. P., Carinhas, N., Carrondo, M. J. T. & Alves, P. M. Insect cells as a production platform of complex virus-like particles. *Expert Rev. Vaccines* **12,** 225–36 (2013).

[4] Lua, L. H. L. *et al.* Bioengineering virus-like particles as vaccines. *Biotechnol. Bioeng.* **111,** 425–440 (2014).

[5] Zhao, Q., Li, S., Yu, H., Xia, N. & Modis, Y. Virus-like particle-based human vaccines: Quality assessment based on structural and functional properties. *Trends Biotechnol.* **31,** 654–663 (2013).

[6] Mateu, M. G. Virus engineering: Functionalization and stabilization. *Protein Eng. Des. Sel.* **24,** 53–63 (2011).

[7] Kaczmarczyk, S. J., Sitaraman, K., Young, H. a, Hughes, S. H. & Chatterjee, D. K. Protein delivery using engineered virus-like particles. *October* **108,** 16998–17003 (2011).

[8] Wu, W., Hsiao, S. C., Carrico, Z. M. & Francis, M. B. Genome-free viral capsids as multivalent carriers for taxol delivery. *Angew. Chemie - Int. Ed.* **48,** 9493–9497 (2009).

[9] Tarasov, S. G. *et al.* Structural plasticity of a transmembrane peptide allows self-assembly into biologically active nanoparticles. *Proc. Natl. Acad. Sci. U. S. A.* **108,** 9798–9803 (2011).

[10] Banerjee, P. S., Ostapchuk, P., Hearing, P. & Carrico, I. S. Unnatural amino acid incorporation onto adenoviral (Ad) coat proteins facilitates chemoselective modification and retargeting of Ad type 5 vectors. *J. Virol.* **85,** 7546–7554 (2011).

[11] Effio, C. L. & Hubbuch, J. Next generation vaccines and vectors: Designing downstream processes for recombinant protein-based virus-like particles. *Biotechnol. J.* (2015).

[12] Thompson, C. M., Petiot, E., Lennaertz, A., Henry, O. & Kamen, A. A. Analytical technologies for influenza virus-like particle candidate vaccines: challenges and emerging approaches. *Virol. J.* **10,** 141 (2013).

[13] Ündey, C., Ertunç, S., Mistretta, T. & Pathak, M. Applied advanced process analytics in biopharmaceutical manufacturing: Challenges and prospects in real-time monitoring and control. *J. Process Control* **20,** 1009–1018 (2010).

[14] Lang, K. & Chin, J. W. Cellular incorporation of unnatural amino acids and bioorthogonal labeling of proteins. *Chem. Rev.* **114,** 4764–806 (2014).

[15] Van Kasteren, S. I., Kramer, H. B., Gamblin, D. P. & Davis, B. G. Site-selective glycosylation of proteins: creating synthetic glycoproteins. *Nat. Protoc.* **2,** 3185–3194 (2007).

[16] Kost, T. A, Condreay, J. P. & Jarvis, D. L. Baculovirus as versatile vectors for protein expression in insect and mammalian cells. *Nat. Biotechnol.* **23,** 567–575 (2005).

[17] Marek, M., Van Oers, M. M., Devaraj, F. F., Vlak, J. M. & Merten, O. W. Engineering of baculovirus vectors for the manufacture of virion-free biopharmaceuticals. *Biotechnol. Bioeng.* **108,** 1056–1067 (2011).

[18] Francis, T., Pearson, H. E., Salk, J. E. & Brown, P. N. Immunity in human subjects artificially infected with influenza virus, type B. *Am. J. Public Health Nations. Health* **34,** 317–334 (1944).

[19] Vicente, T., Peixoto, C., Carrondo, M. J. T. & Alves, P. M. Purification of recombinant baculoviruses for gene therapy using membrane processes. *Gene Ther.* **16,** 766–775 (2009).

[20] Schneider, C. A, Rasband, W. S. & Eliceiri, K. W. NIH Image to ImageJ: 25 years of image analysis. *Nat. Methods* **9,** 671–675 (2012).

[21] Van der Vlist, E. J., Nolte-'t Hoen, E. N. M., Stoorvogel, W., Arkesteijn, G. J. a & Wauben, M. H. M. Fluorescent labeling of nano-sized vesicles released by cells and subsequent quantitative and qualitative analysis by high-resolution flow cytometry. *Nat. Protoc.* **7,** 1311–1326 (2012).

[22] Monteiro, F., Carinhas, N., Carrondo, M. J. T., Bernal, V. & Alves, P. M. Toward system-level understanding of baculovirus-host cell interactions: From molecular fundamental studies to large-scale proteomics approaches. *Front. Microbiol.* **3,** 1–16 (2012).

[23] Stencel-Baerenwald, J. E., Reiss, K., Reiter, D. M., Stehle, T. & Dermody, T. S. The sweet spot: defining virus–sialic acid interactions. *Nat. Rev. Microbiol.* **12,** 739–749 (2014).